

Derivation of novel naive-like porcine embryonic stem cells by a reprogramming factor-assisted strategy

Manling Zhang,^{*,†,‡,§,1} Chenyu Wang,^{*,†,1} Haibin Jiang,^{*,†,1} Manling Liu,^{*,†} Ning Yang,^{*,†}
Lihua Zhao,^{*,†,‡} Daorong Hou,^{*,†} Yong Jin,^{*,†,¶} Qiaoyu Chen,^{*,†} Yuan Chen,^{*,†} Junzheng Wang,^{*,†}
Yifan Dai,^{*,†,‡,2} and Rongfeng Li^{*,†,‡,3}

*Jiangsu Key Laboratory of Xenotransplantation, [†]State Key Laboratory of Reproductive Medicine, [‡]Key Laboratory of Targeted Intervention of Cardiovascular Disease, Collaborative Innovation Center for Cardiovascular Disease Translational Medicine, and [¶]Department of Nephrology, The Affiliated Sir Run Run Hospital, Nanjing Medical University, Nanjing, China; and [§]The State Key Laboratory of Reproductive Regulation and Breeding of Grassland Livestock, Inner Mongolia University, Hohhot, China

ABSTRACT: The establishment of ungulate embryonic stem cells (ESCs) has been notoriously difficult *via* a conventional approach. We combined a traditional ESC culture method with reprogramming factors to assist the establishment of porcine naive-like ESCs (nESCs). Pig embryonic fibroblasts were transfected with a tetracycline-inducible vector carrying 4 classic mouse reprogramming factors, followed by somatic cell nuclear transfer and culturing to the blastocyst stage. Then, the inner cell mass was isolated and seeded in culture medium. The naive-like ESCs had characteristic verys similar to those of mouse ESCs and showed no signs of altered morphology or differentiation, even after 130 passages. They depended on leukemia inhibitory factor signals for maintenance of pluripotency, and the female cell lines had low expression of the X-inactive specific transcript gene and no histone H3 lysine 27 trimethylation spot. Notably, the ESCs differentiated into 3 germ layers *in vitro* and could be induced to undergo directional neural and kidney precursor differentiation under defined conditions, and the ESCs could keep proliferating after doxycycline was removed. nESCs can be established, and the well-characterized ESC lines will be useful for the research of transgenic pig models for human disease.—Zhang, M., Wang, C., Jiang, H., Liu, M., Yang, N., Zhao, L., Hou, D., Jin, Y., Chen, Q., Chen, Y., Wang, J., Dai, Y., Li, R. Derivation of novel naive-like porcine embryonic stem cells by a reprogramming factor-assisted strategy. *FASEB J.* 33, 000–000 (2019). www.fasebj.org

KEY WORDS: inner cell mass · reprogramming factor · pluripotency

Pluripotent stem cells (PSCs) can be classified into 2 distinct and stable pluripotent states: the naive and the primed pluripotent states (1). Naive PSCs correspond to

ABBREVIATIONS: AP, alkaline phosphatase; BMP, bone morphogenetic protein; DOX, doxycycline; EB, embryoid body; ESC, embryonic stem cell; FGF, fibroblast growth factor; FGFR, FGF receptor; H3K27me3, histone H3 lysine 27 trimethylation; ICM, inner cell mass; iPSC, induced PSC; KOSR, knockout serum replacement; bFGF, basic fibroblast growth factors; N2B21, N2 and B27supplement; LIF, leukemia inhibitory factor; LBX, LIF + bFGF + KOSR + N2B27 medium; MEF, mouse embryonic fibroblast; MHC, major histocompatibility complex; LIFR, LIF receptor; nESC, naive-like porcine ESC; OSKM, OCT4, SOX2, KLF4, c-MYC; PEF, pig embryonic fibroblast; pESC, porcine-primed ESC; PSC, pluripotent stem cell; RNA-seq, RNA sequencing; rpESC, reversed-primed porcine ESC; SB, SB431542; SCNT, somatic cell nuclear transfer; Tet, tetracycline; XIST, X-inactive specific transcript

¹ These authors contributed equally to this work.

² Correspondence: Jiangsu Key Laboratory of Xenotransplantation, Nanjing Medical University, Nanjing 210029, Jiangsu, China. E-mail: daiyifan@njmu.edu.cn

³ Correspondence: Jiangsu Key Laboratory of Xenotransplantation, Nanjing Medical University, Nanjing 210029, Jiangsu, China. E-mail: lirongfeng@njmu.edu.cn

doi: 10.1096/fj.201802809R

This article includes supplemental data. Please visit <http://www.fasebj.org> to obtain this information.

the preimplantation of the inner cell mass (ICM) cells of blastocysts, whereas primed PSCs correspond to the postimplantation of epiblasts (1, 2). These 2 types of PSCs show different gene expression profiles and depend on different signaling pathways to support their self-renewal. Naive or authentic embryonic stem cells (ESCs) were first established over 35 yr ago from certain strains of d-3.5 mouse embryos (3, 4). Later, in 2008, authentic rat ESCs were generated with leukemia inhibitory factor (LIF) and signal transduction inhibitors (5, 6). Naive PSCs are characterized by compact dome-like colonies, dependency on LIF, active X chromosomes, and no or very low levels of major histocompatibility complex (MHC) class-I antigen expression (7). Naive PSCs are also tolerant to passage as single cells and show no signs of either senescence or overextended culture doublings. They have the ability to differentiate, both *in vitro* and *in vivo*, into multiple cell types that represent the 3 germ layers, and they contribute to the germ line in chimeric offspring. By contrast, conventional human and monkey ESCs appear to resemble a primed pluripotent state because they share many characteristics with mouse epiblast stem cells (8–12). Primed PSCs form flat colonies, depend on basic fibroblast growth

factor (bFGF) (1), and have an inactivated X chromosome. They show positive expression of MHC class-I antigen, intolerance to single cell passage, and very limited capacity to contribute to chimeric offspring.

Many researchers have attempted to establish ESCs from porcine embryos because the pig is recognized as an ideal experimental animal in human medical research and is a close match for humans in terms of anatomy and physiology (13). Attempts to derive porcine ESCs began at least 25 yr ago (14–16), and most researchers have used methods similar to those employed initially in the mouse (3). The resulting cells have shown some measure of stemness, including an ability to be maintained in culture for prolonged periods (15), to form teratomas and, in one instance, to give rise to chimeras (17). The established pluripotent cell lines, like those from human blastocysts, clearly fall into the primed ESC class, and their existence underscores the commonality of the FGF2-dependent pluripotent state. Some researchers have derived porcine PSCs using small molecular inhibitors. For example, Haraguchi *et al.* (13) generated self-renewing porcine embryonic stem-like cells from the ICM of porcine embryos using the inhibitors CHIR99021 and PD184352. Similarly, Telugu *et al.* (18) derived LIF-dependent, so-called naive-type PSCs from porcine embryos by up-regulating the expression of KLF4 and OCT-4 in the ICM with lentivirus vector, followed by culture in medium containing ken-pauillone and CHIR99021. A number of recent studies have also reported the generation of putative naive human PSCs (hPSCs) that molecularly resemble mouse ESCs (mESCs) (19–21). The study by Gu *et al.* (22) showed that human ESCs in the primed state can be converted to the naive-like state by cultivation under optimizing culture conditions, namely LBX medium (LIF + bFGF + KOSR + N2B27), and this culture medium could also generate porcine induced PSCs (iPSCs) that resemble mESCs (23). Therefore, although many researchers have attempted to derive porcine ESCs, the establishment of well-defined naive ESCs has not yet been achieved.

Here, we used the strategies of ESC culture methods in combination with iPSC techniques to derive porcine naive-like ESCs (nESCs). Pig embryonic fibroblasts (PEFs) were first transfected with a tetracycline (Tet)-inducible vector carrying the 4 classic mouse (m) reprogramming factors mOCT4 (POU5F1), mSOX2, mKLF4, and mc-MYC (mOSKM), followed by somatic cell nuclear transfer (SCNT) and culture to the blastocyst stage at d 6. The ICMs were then seeded on mouse embryonic fibroblasts (MEFs) that had been cultured with LBX medium containing the small molecular inhibitors CHIR99021, PD0325901, and SB431542 (SB). The resulting nESCs were confirmed pluripotent by thorough investigation, and they possessed many characteristics very similar to those of mouse ESCs.

MATERIALS AND METHODS

Chemicals

All chemicals were purchased from MilliporeSigma (Burlington, MA, USA) and Thermo Fisher Scientific unless otherwise indicated.

Donor cell preparation

PEFs were isolated from d-35 porcine fetuses. Primary cells were transfected with a Tet-inducible vector carrying the 4 classic mouse reprogramming factors (mOSKM) and then screened with antibiotics. Before SCNT, a suspension of single cells was prepared in a manipulation medium (25 mM HEPES-buffered tissue culture medium 199 containing 3 mg/ml bovine serum albumin).

In vitro maturation of oocyte and embryo production

Porcine ovaries (gilts) were collected from a local slaughterhouse. The cumulus-oocyte complexes were aspirated, collected, and transferred to an *in vitro* maturation medium at 38.5°C in an atmosphere of 5% CO₂ in air. After 42–44 h of maturation culturing, the cumulus-oocyte complexes were transferred to Tyrode's Albumin Lactate Pyruvate (TL)-HEPES buffer containing 0.1% hyaluronidase (w/v) and vortexed to remove the cumulus cells.

Matured oocytes with the first polar body were transferred into the manipulation medium supplemented with 7 µg/ml cytochalasin B. The polar body, along with a portion of the adjacent cytoplasm, was removed, and a donor cell was placed in the perivitelline space. The reconstructed embryos were then cultured in porcine zygote medium-3 (PZM-3) medium until fusion and activation were achieved.

Establishment and culture of nESCs

The embryos were cultured to the early blastocysts stage for 6 d. The zona pellucidae of blastocysts were removed by treatment in 0.5% pronase solution for 10 s. Blastocysts were then incubated in 10% rabbit anti-porcine serum for 30 min and 10% guinea pig complement for 30 min. The ICMs were isolated from lysed trophoblast cells and seeded onto a monolayer of mitomycin C-inactivated MEFs at a density of 1×10^5 cell/well. The MEFs were inactivated with 10 µg/ml mitomycin C for 2.5 h, resuspended, and seeded in 4-well dishes precoated with 0.1% gelatin. The nESCs medium was LBX medium with added knockout serum replacement (KOSR) medium and N2B27 medium and supplemented with 16 ng/ml FGF, 2000 U/ml LIF, and 2 µg/ml doxycycline (DOX). The KOSR medium was knockout DMEM supplemented with 20% KOSR, 1% NEAA, 2 mM L-glutamine, 1% PS, 0.1 mM β-mercaptoethanol, 3 µM CHIR99021, 1 µM PD0325901, 2 µM SB, and 50 ng/ml Vitamin C (VC). The N2B27 medium was DMEM/F12 medium and Neurobasal supplemented with 1% N₂, 2% B27, 0.25 mg/ml bovine serum albumin, 5 µg/ml insulin, 1% PS, 3 µM CHIR99021, 1 µM PD0325901, 2 µM SB, and 50 ng/ml VC. The ICMs were cultured at 38.5°C in a 5% CO₂ atmosphere. The culture medium was changed 2 d after the blastocysts were transferred to the ESC medium and then changed every day.

Karyotyping

The chromosomes of established nESC lines 1, 2, 3, and 4 were analyzed at passages 28, 27, 36, and 39, respectively. The cells were incubated in a medium supplemented with 0.02 µg/ml colcemide for 1 h at 38.5°C in an atmosphere of 5% CO₂ in air. After trypsinization and treatment with hypotonic KCl (0.56%) for 30 min, the cells were fixed with a 3:1 (v/v) mixture of methanol and acetic acid and spread on clean microscopic slides by gentle dropping. After staining with Giemsa (1:10 dilution) for 20 min, the chromosomes were examined at ×1000 magnification.

Alkaline phosphatase staining and immunocytochemistry

Alkaline phosphatase (AP) activity of the nESC line 1 at different passages was assayed with an AP detection kit (MilliporeSigma) according to the manufacturer's instructions. For immunofluorescence staining, the nESC lines 1 and 3 were cultured on coverslips and fixed with 4% paraformaldehyde for 10 min, permeabilized with 1% Triton X-100 for 1 h, and blocked with 10% goat serum for 1 h at room temperature. The cells were then incubated with primary antibodies at 4°C overnight and incubated with secondary antibodies for 1 h at room temperature. The primary antibodies included OCT4 (Santa Cruz Biotechnology, Dallas, TX, USA), SOX2 (Calbiochem, San Diego, CA, USA), NANOG (Santa Cruz Biotechnology), KLF4 (MilliporeSigma), SSEA-1 (Novus Biologicals, Centenniel, CO, USA), desmin (MilliporeSigma), cytokeratin (MilliporeSigma), neurofilament (MilliporeSigma), β III-tubulin (Cell Signaling Technology, Danvers, MA, USA), WT1 (Abcam, Cambridge, MA, USA), and histone H3 lysine 27 trimethylation (H3K27me3) (Santa Cruz Biotechnology). Secondary antibodies include goat anti-mouse IgG Alexa Fluor 546 (Thermo Fisher Scientific) and goat anti-rabbit IgG rhodamine (Rockland Immunochemicals, Limerick, PA, USA). The nuclei were stained with DAPI, and the stained cells were examined using a confocal imaging system (710; Carl Zeiss, Oberkochen, Germany). The image acquisition, analysis, and processing were standardized within each experiment.

PCR analysis and Western blotting

Total RNA was extracted from cultured nESC lines 1, 2, 3, and 4 using Trizol, and cDNA was synthesized using a QuantiTect Reverse Transcription Kit (Vazyme, Nanjing, China). The sequences of the primers and annealing temperatures used were listed in Supplemental Table S1. Real-time RT-PCR analysis was also performed as previously described by Ezashi *et al.* (24).

Western blotting was performed according to methods described by Haraguchi *et al.* (13).

Embryoid body formation and directed differentiation of nESCs under chemically defined conditions

For embryoid body (EB) formation, colonies of nESC line 1 were trypsinized into single cells and cultured in hanging drops in LBX medium without bFGF, LIF, and small molecular inhibitors for 5 d. The EBs were subsequently placed on dishes coated with gelatin and cultured in the same conditions for an additional 5 d. The 3 germ layers and associated genes and markers were detected by RT-PCR and immunocytochemistry, respectively.

The nESCs from line 1 were tested for their potential to differentiate into defined lineages under chemically defined medium conditions in the absence of DOX support. They were differentiated into a mesodermal lineage following 12 d of culture as previously described by Takasato *et al.* (25) and differentiated into a neuronal lineage by culturing for 5 d in neural differentiation medium in the presence of 1 mg/ml heparin on a gelatin-coated dish (26).

Analysis of signaling dependence

For LIF signal pathway identification, nESCs from line 3 were cultured in medium with different concentrations of LIF (0, 500, 1000, 1500 and 2000 U/ml) for 3 d, and the total number of AP-positive clones was calculated. The cells were also seeded in

gelatin-coated feeder-free wells and cultured in medium with or without LIF, supplemented with 1 or 10 μ M JAK inhibitor SD1008 (Tocris Bioscience, Bristol, United Kingdom). After treatment for 3 d, the morphologic changes in the cells were evaluated.

For FGF signal pathway identification, nESCs from line 1 were cultured in medium with different concentrations of bFGF (0, 4, 8, 12, 16, 20, and 24 ng/ml) for 3 d, and the total number of AP-positive clones was calculated. The cells were also cultured in medium supplemented with or without 2 μ M FGF receptor (FGFR) inhibitor SU5402 (Tocris Bioscience) for 3 d, and then the total number of AP-positive clones was calculated.

MicroRNA expression analysis by microarray

For microRNA analysis, total RNA from nESC line 1 at passage 13, nESC line 2 at passage 14, pESCs at passage 19 (established previously in our laboratory), ICMs, and PEFs were extracted with Trizol Reagent (Takara, Kyoto, Japan) according to the manufacturer's instructions. The PEFs served as a negative control, and the ICMs served as a positive control. MicroRNA expression profiles (microarray analysis) were obtained from the ESCs using the Affymetrix Gene Chip Porcine 3 Expression and Porcine Gene 1.0 ST Array (Thermo Fisher Scientific), which is based on the Sscrofa9 (susScr2) database (<https://www.cepbrowser.org/cgi-bin/hgGateway>). Differentially expressed microRNAs were identified through fold changes as well as by *P* values calculated with the Student's *t* test, and hierarchical clustering was performed to display the distinguishable microRNA expression patterns among the samples.

Transcriptional profiling expression analysis by RNA sequencing

For RNA sequencing (RNA-seq), a total amount of 3 μ g RNA per sample from nESC line 1 at passage 24, nESC line 3 at passage 24, nESC line 1 at passage 27 cultured without DOX, porcine iPSC line 2 at passage 20, ICM, and PEF were used as input materials for the RNA sample preparations. The RNA-seq libraries were generated using the rRNA-depleted RNA by NEBNext Ultra Directional RNA Library Prep Kit for Illumina following the manufacturer's recommendations (New England Biolabs, Ipswich, MA, USA). The RNA-seq libraries were sequenced on a HiSeq4000 platform. The top 90% expressed genes [\log_2 (normalized counts)] in the whole RNA-seq data set were used for clustering analysis. Transcripts with a *P* adjust < 0.05 were assigned as differentially expressed.

RESULTS

Isolation and establishment of nESCs

To establish different lineage nESCs, the female and male PEFs carrying both Tet-inducible vector and the mOSKM were used as donor cells to produce SCNT embryos. ICMs from d-6 blastocysts (Fig. 1A) were freed of trophectoderm by immunosurgery (Fig. 1B) and then placed on the mitomycin C-treated MEFs. After 2–3 d of culturing, the ICMs began to attach on the feeder cell layer (Fig. 1C), and 4–7 d later they formed the first outgrowth (Fig. 1D). The attachment and outgrowth percentages were 22.8% (29/127) and 34.5% (10/29), respectively. The outgrowths were routinely mechanically passaged by aspirating the colonies into fine pipettes, and 3 d later, the colonies were

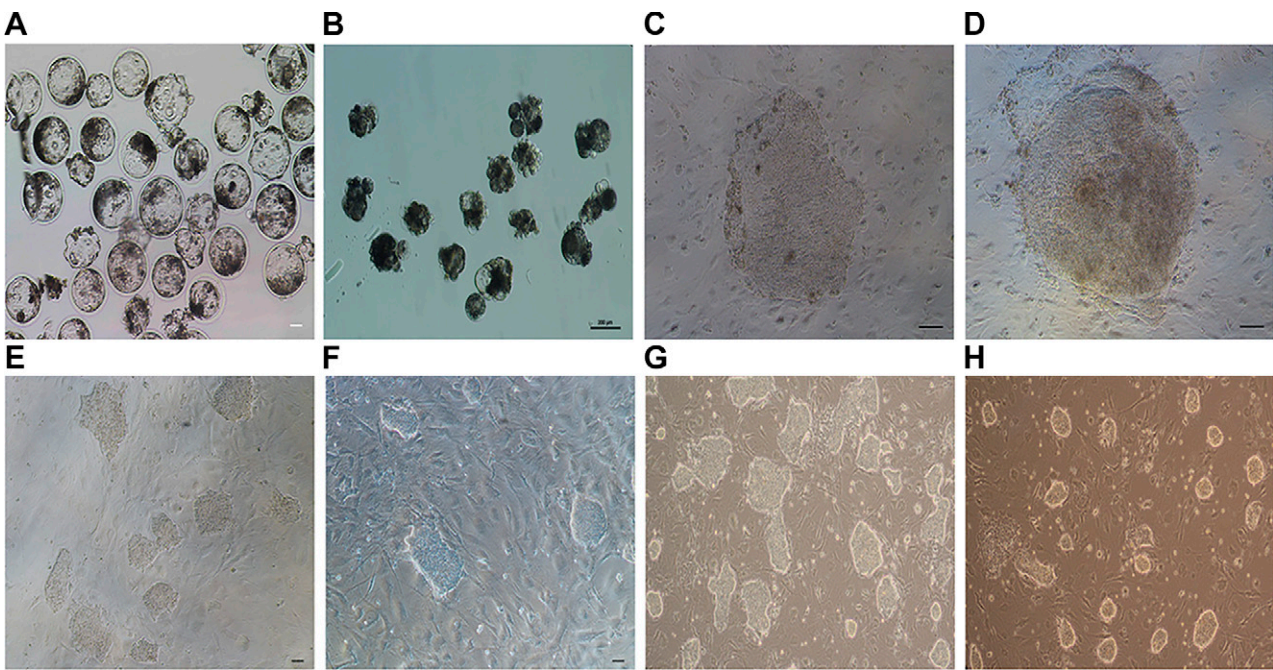


Figure 1. Derivation and morphology of nESCs. *A*) SCNT blastocysts at d 6. *B*) Blastocysts after immunosurgery treatment. *C, D*) The d-6 and d-8 attached ICM. *E–H*) The morphology of nESCs colony at passages 11, 20, 32, and 50. Scale bars, 100 μ m.

passaged for 5 passages by dissociation with collagenase for 20 min and then 0.25% trypsin for 2 min. We then routinely passaged these cells into single cells every 3–4 d using 0.25% trypsin and plating them into wells pre-seeded with MEFs.

Two female nESC lines (named nESC1 and 2) and 2 male nESC lines (named nESC3 and 4) were established and cultured for 139, 97, 110, and 68 passages and still maintained vigorous growth. The colonies exhibited a compact, dome-like morphology at different passages (Fig. 1*E–H*) and had a cell growth curve (Supplemental Fig. S1) similar to that of mESCs. The established cell lines could be cryopreserved and recovered with high efficiency using standard techniques.

The pluripotent states of nESCs

These established nESC lines exhibited many characteristics near to naive pluripotency. The cells exhibited positive staining for AP at different passages (Fig. 2*A*), and immunofluorescence analysis confirmed that they expressed the pluripotency markers OCT4, NANOG, SOX2, and KLF4 in their nuclei and SSEA-1-positive expression in cytomembrane (Fig. 2*B* and Supplemental Fig. S2). The specific staining of antibodies was also demonstrated (Supplemental Fig. S3).

The exogenous genes of mouse OSKM and endogenous genes of pig OSKM were both detected by RT-PCR (Fig. 3*A*). The female or male cells displayed a continued normal 38XX or 38XY karyotype at different passages (Fig. 3*D* and Supplemental Fig. S4). The RNA transcripts of pluripotency markers, including OCT4, NANOG, SOX2, c-MYC, LIN28, TBX3, and DPPA5, were detected in nESCs by RT-PCR (Fig. 3*B*). Western blotting analysis further verified the expression of pluripotent markers OCT-4,

SOX2, NANOG, and SSEA-1 (Fig. 3*E*). Gray-scale analysis showed the same results (Student's *t* test, $P < 0.05$) (Fig. 3*G*). No or low levels of MHC class-I expression is another hallmark of the naive state (7), and the nESCs were negative for MHC class I as assessed by RT-PCR (Fig. 3*C*). The LIF signal pathway-related genes, including LIF, gp130, LIF- α , and LIF- β , were detected in nESCs by RT-PCR (Fig. 3*B*). Protein STAT3 phosphorylation is also an important mark for the activated LIF signal pathway (27), and LIF dependence was confirmed by detection of phosphorylated STAT3. Western blotting showed that phosphorylation of STAT3 occurred in nESCs and mESCs but not in hESCs (Fig. 3*F*).

Both X chromosomes are active in female ESCs, and expression of the X-inactive specific transcript (*XIST*) gene was lower in naive PSCs (1). Culturing of the female nESCs in α -MEM medium with FGF and activin resulted in loss of the dome-like morphology, and the cells became flat. We called these cells reversed-primed ESCs (rpESCs). Real-time RT-PCR analysis showed an increased expression of the *XIST* gene in the rpESCs compared with the nESCs (Fig. 3*H*) (Student's *t* test, $P < 0.05$). The staining of H3K27me3, which is associated with the inactive X chromosome, further indicated a greater accumulation of H3K27me3 in rpESCs than in nESCs because of the reduced or absent H3K27me3 spot in nESCs (Fig. 3*I*).

We further investigated the response of the cells to different signaling inhibitors. The percentage of AP-positive cell colonies obviously decreased with removal of LIF from the medium. Because LIF is the key cytokine secreted by feeder cells (MEF), this may mask any effects of exogenous addition of the factor. Therefore, we plated nESCs onto gelatin-coated dishes in LBX medium, LBX medium without LIF, LBX medium with 1 μ m added SD1008 (an inhibitor of JAK or STAT3), and LBX medium

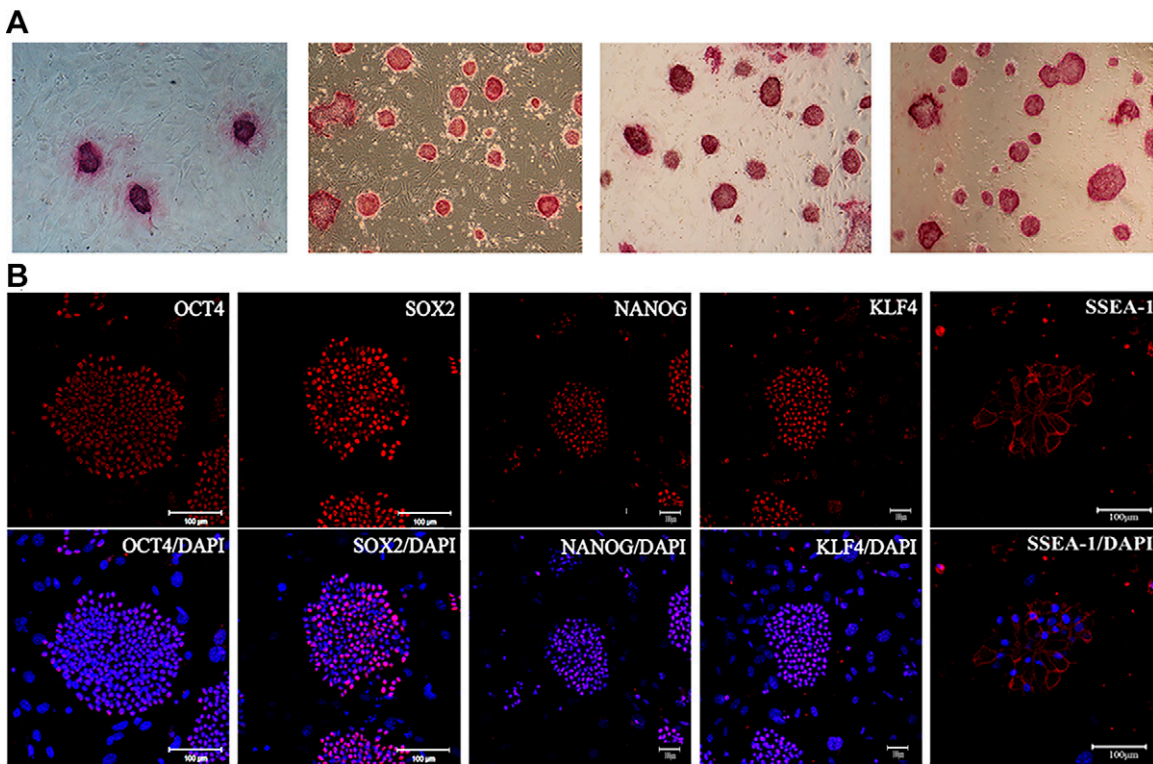


Figure 2. Characteristics of nESCs. *A*) AP staining of nESC at passage 11, 24, 38, and 54. *B*) The immunofluorescence staining of pluripotency markers NANOG, OCT4, KLF4, SOX-2, and SSEA-1 in nESC line 1 colonies (at passage 28) cultured on MEF cells. Scale bars, 100 μ m.

with 10 μ M added SD1008. In the presence of LIF, ~10–20% of the cells remained undifferentiated after 2 passages in culture; however, all the cells differentiated rapidly when exposed to a JAK or STAT3 inhibitor or following removal of LIF, and the cells could not be maintained beyond 1 passage (Fig. 4A, B). This indicated that the self-renewal of nESCs depended on LIF signaling. Removal of FGF from the medium significantly increased the percentage of AP-positive cell colonies (Fig. 4C). In the presence of the FGFR inhibitor SU5402, the percentage of AP-positive cell colonies was nearly equal to that obtained in the absence of SU5402 (Fig. 4D). The cells cultured with different concentrations of FGF could be passaged normally, but the cell number decreased when the concentration of FGF was reduced in the medium (Fig. 4E), indicating that the self-renewal of nESCs did not depend on FGF signaling; however, inclusion of FGF could improve cell proliferation.

Multilineage differentiation of nESCs

The classic method for inducing ESC differentiation is to allow ESCs to grow in suspension and form 3-dimensional aggregates known as EBs (28). Within the EBs, ESC differentiation proceeds on a schedule similar to that in the embryo. The nESCs could form EBs when grown in suspension without LIF, FGF, and small molecules for 5 d (Fig. 5A). We plated d-4 EBs onto gelatin-coated dishes under the same conditions, and the cells in the outgrowth of EBs displayed the morphology of distinct differentiation (Fig. 5B). Immunocytochemical analysis confirmed the

expression of differentiation markers for ectoderm (neurofilament), endoderm (cytokeratin 17), and mesoderm (desmin) in these differentiated cells (Fig. 5C).

The nESCs could also be induced to undergo successful differentiation under defined conditions. They differentiated into kidney precursors when cultured in defined medium without DOX for 12 d (Fig. 5E). The expression of the intermediate mesoderm-related genes OSR1, PAX2, and LHX1 were detected by RT-PCR when differentiated at d 6 (Supplemental Fig. S5A), and RT-PCR confirmed the expression of the metanephric mesenchyme and primitive streak stage-related genes WT1, GDNF, SIX2, OSR1, PAX2, HOXB7, and HOXD11 when the cells were differentiated at d 12 (Supplemental Fig. S5B). Real-time RT-PCR analysis showed that the expression of these kidney precursor-related gene was significantly increased when cells were differentiated at d 6 and 12 compared with undifferentiated cells at d 0 (Student's *t* test, $P < 0.05$) (Fig. 5D). Immunofluorescence analysis confirmed that cells were WT1-positive (Fig. 5F) when they were differentiated at d 12. Western blotting and Gray-scale analysis further verified the expression of WT1 in differentiated cells (Student's *t* test, $P < 0.05$) (Fig. 5G). The nESCs differentiated into neuroectodermal precursors under defined medium without DOX for 5 d (Fig. 5I). RT-PCR confirmed the expression of the neuron-related genes CD4, GBBR1, and NEUROD1, the astrocyte-related genes SPARC, GLUL, and GFAP, and the synapse-related genes PLP1 and TF (Supplemental Fig. S5C) when the cells were differentiated at d 5. Real-time RT-PCR analysis showed that the expression of these neural related genes was

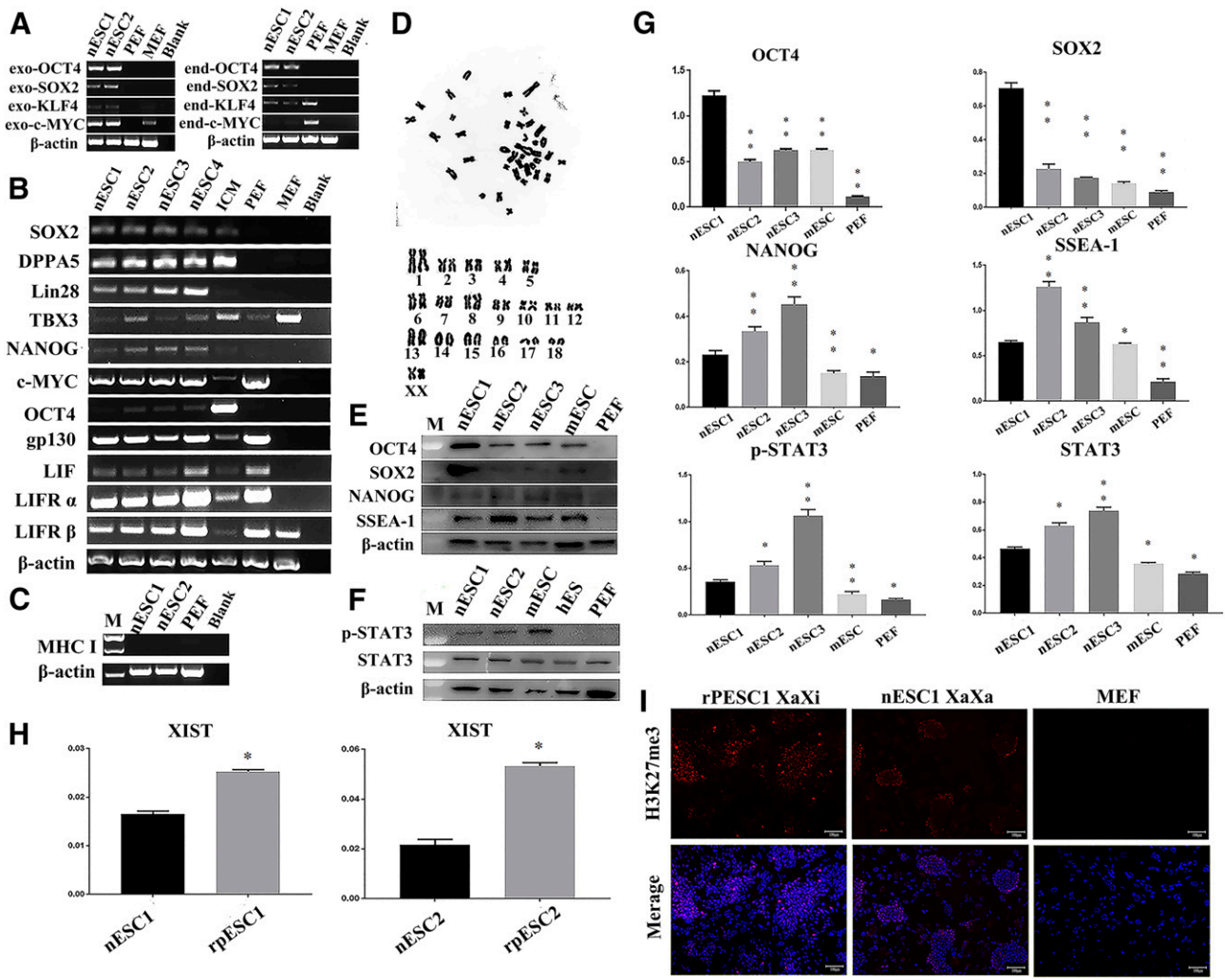


Figure 3. Characteristics of nESCs. *A*) RT-PCR analysis of exogenous and endogenous pluripotent genes of OCT-4, SOX-2, KLF-4, and c-MYC in nESC lines 1 and 2 at passages 14 and 15. end, endogenous; exo, exogenous. *B*) RT-PCR analysis of relative transcript concentrations of pluripotent and lineage-specific genes in nESC lines 1, 2, 3, and 4 at passages 14, 15, and 12, respectively, and in ICM, PEFs, and MEFs. *C*) RT-PCR analysis of MHC-1 gene in nESC lines 1 and 2 at passages 14 and 15. *D*) Karyotype analysis of nESC line 1 at passage 28. *E*) Western blotting analysis confirming the expression of pluripotent genes in the nESC lines 1, 2, and 3. Lysates from mouse ESCs and PEFs were used as positive and negative controls, respectively. *F*) Phosphorylation status of STAT3 in the nESC lines 1 and 2 at passages 45 and 44. mESCs and hESCs were used as controls. p-STAT3, phosphorylated STAT3. *G*) Gray value analysis of Western Blotting. *H*) Quantitative RT-PCR for the XIST gene. The expression of the xist gene in nESC lines 1 and 2 at passages 21 and 18 and their rpESCs cultured for 3 passages was compared. *I*) Immunostaining for H3K27me3 in rpESCs and nESCs; histone H3K27 trimethylation spots were observed in rpESCs but not in nESCs. End, endogenous; exo, exogenous; p, phosphorylated; XaXa, active X chromosome; XaXi, inactivated X chromosome. Data are depicted as mean \pm SD. Scale bars, 100 μ m. * P < 0.05. ** P < 0.01.

significantly increased when cells were differentiated at d 5 compared with undifferentiated cells at d 0 (Student's *t* test, P < 0.05) (Fig. 5*H*). Immunofluorescence analysis showed that cells were β III-tubulin-positive when they were differentiated at d 5 (Fig. 5*J*). Western blotting and Gray-scale analysis further verified the expression of β III-tubulin in differentiated cells (Student's *t* test, P < 0.05) (Fig. 5*K*).

Comparison of reprogramming factor expression in the nESCs

The expression levels of the transgenes and the endogenous OSKM were investigated by quantitative RT-PCR. Expression of endogenous pSOX2 and pc-MYC in the naive-like

ESC line 1 increased significantly (Student's *t* test, P < 0.01) (Fig. 6*B*), and that of the exogenous OSKM decreased significantly (Student's *t* test, P < 0.01) (Fig. 6*A*) after the gradual removal of DOX from the medium (2, 1, 0.5, 0 μ g/ml). In addition, expression of the exogenous OSKM was significantly lower (Student's *t* test, P < 0.01) in the nESC line 1 than in the iPSCs (Fig. 6*C*) derived from PEFs following induction with the same 4 reprogramming factors and using the same culture system. The expression of endogenous pSOX2, pKLF4, and pc-MYC was significantly higher (Student's *t* test, P < 0.05) in the nESC line 1 than in the iPSCs (Fig. 6*D*).

In order to obtain porcine ESCs without exogenous transcriptional factor expression, we simultaneously cultured nESC line 1 and nESC line 4 in LBX medium without

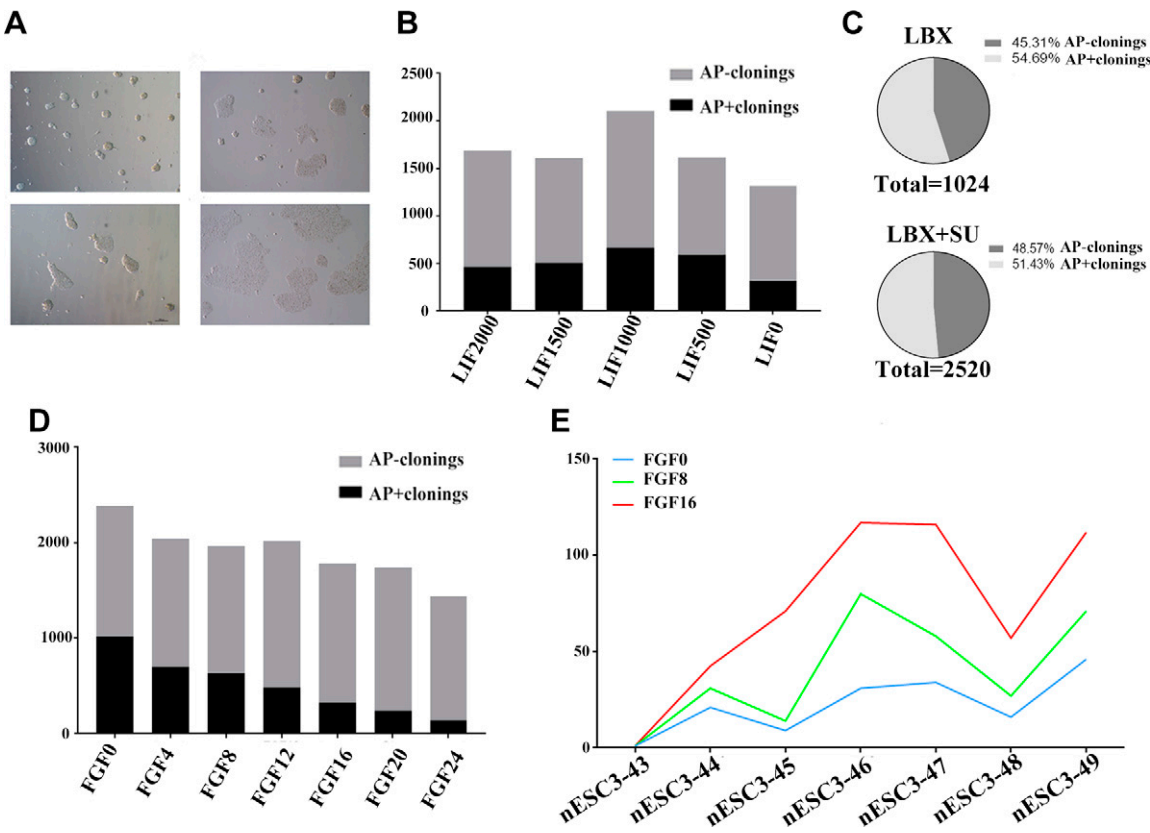


Figure 4. Signaling dependence analysis of nESCs. *A*) The morphology of nESCs cultured in LBX, LBX without LIF, LBX + 1 μ M SD1008, and LBX + 10 μ M SD1008. Scale bars, 100 μ m. *B*) The AP-positive colonies rate of nESCs culture with different concentration of LIF. *C*) The positive rate of AP staining of nESCs cultured with different concentration of bFGF. SU, FGF receptor inhibitor SU5402. *D*) The positive rate of AP staining of nESCs cultured with or without 2 μ M FGFR inhibitor SU5402. *E*) Cell counting of nESCs cultured with different concentration of bFGF in different passage.

FGF and DOX. The nESC line 1 gradually died after 2 generations of culture, whereas the nESC line 4 survived 10 generations of culture and could be passaged normally. Total RNA was extracted from nESC line 1 at passage 14 cultured with DOX and at passage 29 after 2 passages without DOX; RNA was also extracted from nESC line 4 at passage 21 cultured with DOX and at passages 33, 37, and 41 after 2, 6, and 10 passages without DOX. T vector polyA (TA) cloning sequencing showed that the 4 transcriptional factors were continuously expressed in different proportions in both cell lines, but the expression of the exogenous SOX2 decreased significantly, especially in the nESC line 4 after 2 passages without DOX, where expression of exogenous SOX2 was completely eliminated (Fig. 6E and Supplemental Fig. S6).

MicroRNA and mRNA expression of nESCs by microarray and RNA-seq analysis

The microRNA expression of nESC lines 1 and 2 was compared with porcine primed ESCs (pESCs), ICMs, and PEFs using the Affymetrix Gene Chip Porcine 3 Expression and Porcine Gene 1.0 ST Array. Tree groups could be identified in the heatmap. Hierarchical clustering result showed the microRNA expression pattern of nESCs was more similar to that of ICMs and pESCs than to that of PEFs (Fig. 7A). The microarray data revealed significantly

higher expression of about 8 microRNAs, including microRNA-28-3p (miR-28-3p) and microRNA-205(miR-205) (higher in ICMs than in nESCs), and of about 7 microRNAs, including miR-205 and microRNA-4334-5p (miR-4334-5p) (higher in ICMs than in pESCs) (Supplemental Table S2). Expression of miR-28-3p, miR-205, and microRNA-3613 (miR-3613) in ICM, pESCs, and nESCs decreased progressively. In particular, the expressed quantity of miR-205 in ICM was about 89 times more than in nESC line 1, 285 times more than in nESC line 2, and 473 times more than in pESCs.

To investigate the molecular features of nESCs, we profiled their transcriptome by RNA-seq and compared this with the transcriptomes of porcine iPSCs, ICM, and PEF; we also compared the nESCs cultured without DOX. Hierarchical clustering results showed that nESC line 1 and iPSCs cluster together, whereas nESCs cultured without DOX were close to ICM (Fig. 7B); this indicated that the nESCs tend to turn into ESCs in the absence of DOX and change to iPSCs in the presence of DOX.

We also selected some typical pluripotency genes and compared the expression levels of these genes in nESCs with expression in iPSCs, ICMs, and PEFs (Fig. 7C). Most pluripotency genes were expressed at lower levels in nESCs than in ICM; these genes include *OCT-4*, *REX1* (*ZFP42*), *KLF4*, *KLF5*, *TBX3*, *DPPA5(Esg1)*, *SALL4*, *TFCP2L1*, and *PECAM1*. However, expression of the

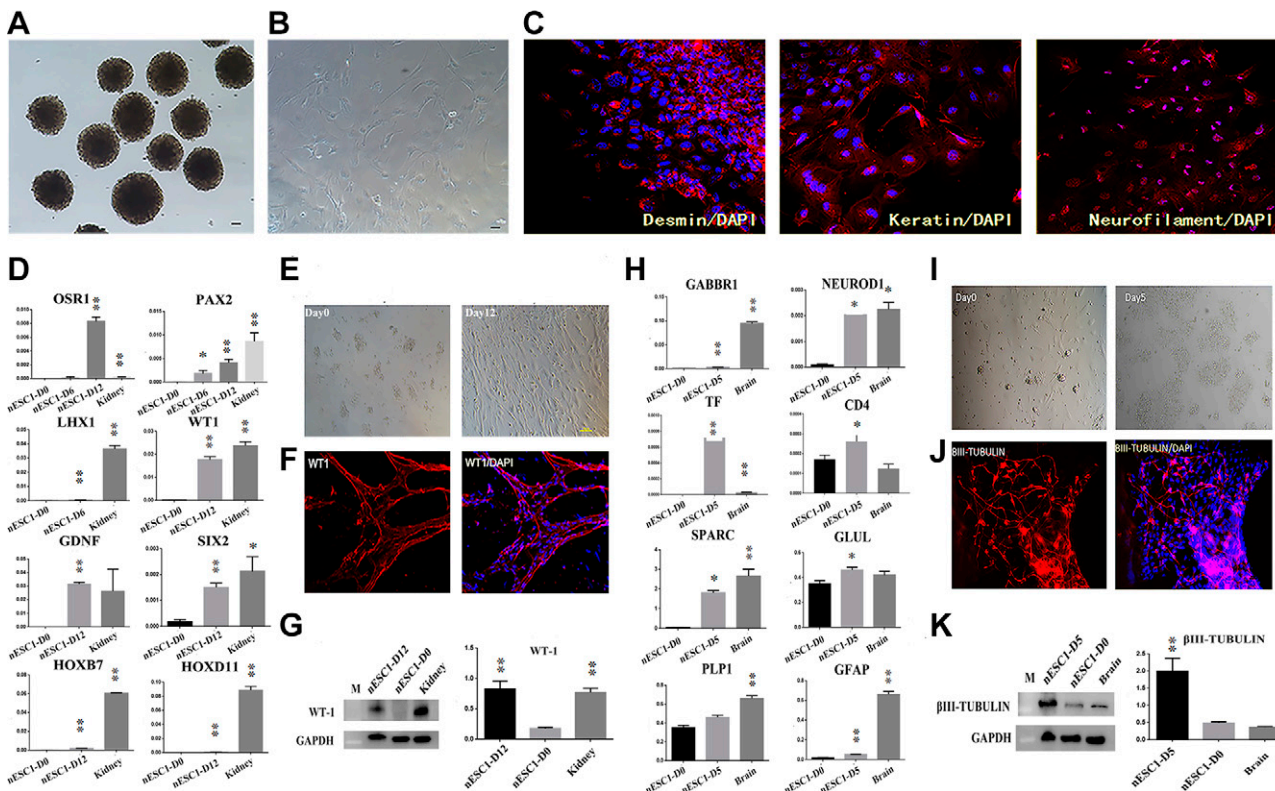


Figure 5. *In vitro* differentiation potential of nESCs. *A*) EB derived from nESCs of line 1 at passage 14. *B*) EB spread on dishes coated with gelatin displayed distinct signs of differentiation. *C*) Expression of differentiation marker cytokeratin 17 (endoderm), desmin (mesoderm), and neurofilament (ectoderm) from differentiated nESCs was confirmed by immunocytochemistry analysis. *D*) Quantitative RT-PCR for the intermediate mesoderm, metanephric mesenchyme, and primitive streak stage-related genes in nESCs differentiated at d 0, 6, and 12. *E*) The difference between cells differentiated at d 0 and 12 can be clearly seen under the microscope. *F*) Expression of differentiation marker WT1 at d 12 from differentiated nESCs was confirmed by immunofluorescence analysis. *G*) Western blotting analysis confirming the expression of WT1 in differentiated nESCs and the gray value analysis. *H*) Quantitative RT-PCR for the neuron-, astrocyte-, and oligodendrocyte-related genes in nESCs differentiated at d 0 and 5. *I*) The difference between cells differentiated at d 0 and 5 can be clearly seen under the microscope. *J*) Immunofluorescence staining of d-5 neural differentiation cultures showed that cells at d 5 were positive for the postmitotic neuron marker βIII-tubulin. *K*) Western blotting analysis confirming the expression of βIII-tubulin in differentiated nESCs and the gray value analysis. Brain, positive control with pig brain; GAPDH, glyceraldehyde 3-phosphate dehydrogenase as control for normalization; kidney, positive control with pig kidney. Data are depicted as mean \pm SD. Scale bars, 100 μm. * $P < 0.05$. ** $P < 0.01$.

pluripotency genes, such as *OCT4*, *SUZ12*, *SOX2*, *LIN28A*, *NR6A1*, *PODXL*, *GNL3*, *AVCR2B*, *UTF1*, *ESRRB*, and *CDH1*, was significantly higher in nESCs than in PEFs. Some pluripotency genes, such as *KLF4*, *SUZ12*, *PECAM1*, *REX1*, and *ID1*, were expressed at higher levels in nESCs than in iPSCs. In particular, some pluripotency genes, such as *SOX2*, *STAT3*, *LIN28A*, *NR6A1*, *SMAD2*, *SMAD3* and *TERT*, were expressed at higher levels in nESCs than in ICM. The RNA-seq data indicated a much higher expression of the core stem cell transcription factors *OCT4*, *KLF4*, *REX1*, *TBX3*, and *DPPA5* in ICM than in nESCs (Supplemental Table S3). Collectively, these data indicated that the gene expression pattern of nESCs was distinct from that of PEFs, and the nESCs may possess characteristics that resemble both ESCs and iPSCs.

DISCUSSION

In this study, nESCs morphologically similar to mouse ESCs were isolated from SCNT embryos. We established 4

cell lines that could be propagated rapidly without any overt change in morphology, even after 130 passages. Our results demonstrate that the use of LBX medium enables the efficient derivation and maintenance of cells from porcine blastocysts that show some key features of ESCs: expression of the pluripotency markers *OCT4*, *NANOG*, *KLF4*, *SOX2*, and *SSEA-1*; long-term self-renewal; the capacity to differentiate into all 3 germ layers; and the capacity for digestion into single cells.

A number of attempts to generate ESCs in porcine have been reported; however, the characterization results have not been as definitive as those from mice. Some researchers reported the establishment of ESC-like cells from pigs; however, they were not able to subculture beyond 20 passages (29–33). In addition, the vast majority of these studies showed that the derived pluripotent cells were the primed type, and most studies used the nonenzymatic passaging methods to passage the cells (27, 34). As far as we know, only Telugu *et al.* (18) derived a LIF-dependent cell line by ectopic overexpression of *KLF4* and *OCT4* in ICMs of porcine blastocysts, and their putative naive

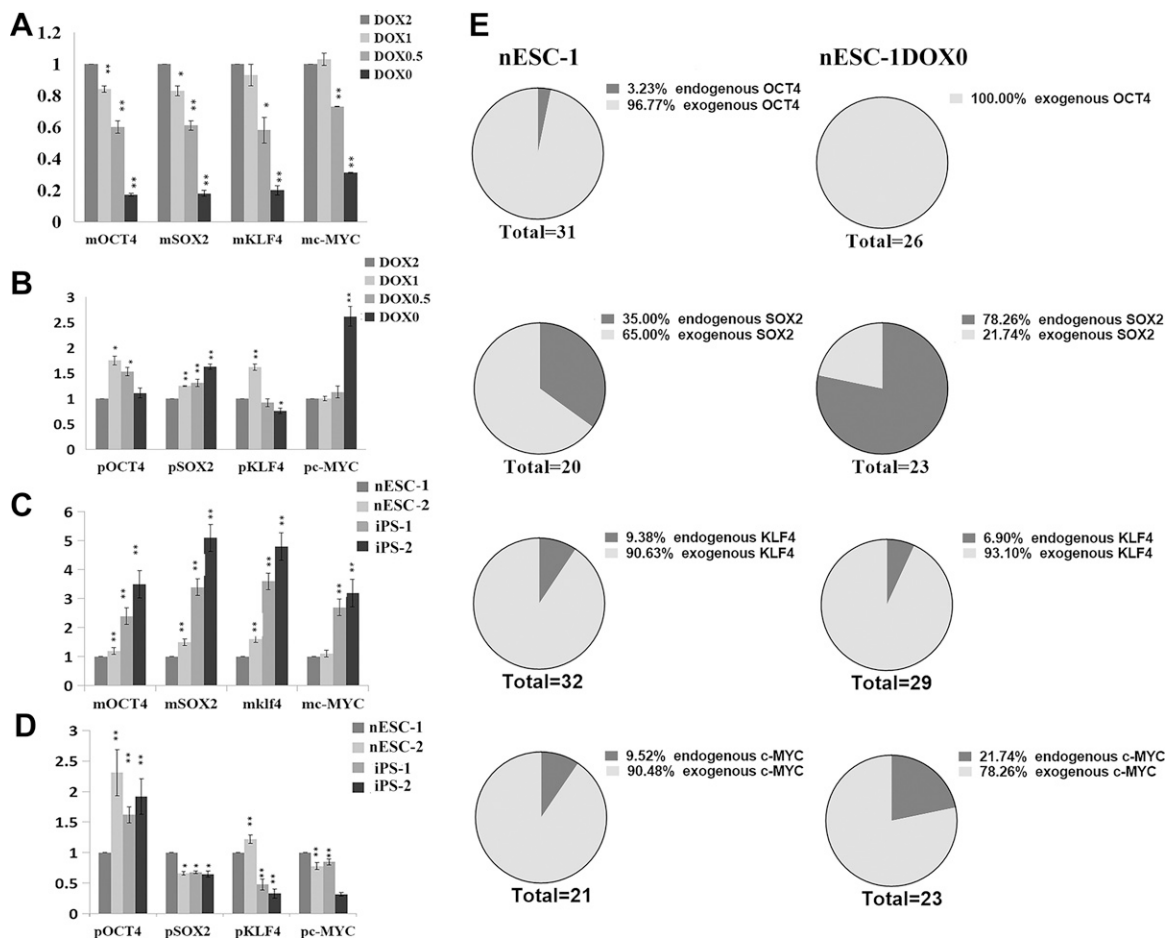


Figure 6. The analysis of pluripotent genes of OCT-4, SOX-2, KLF-4, and c-MYC in nESCs. *A, B)* Real-time RT-PCR analysis of the exogenous and endogenous pluripotent genes in the nESCs treated with different concentrations of DOX. *C, D)* Real-time RT-PCR analysis of the exogenous and endogenous pluripotent genes in the nESCs and iPSCs. *E)* The expression of endogenous and exogenous pluripotent genes from nESC line 1 in the LBX medium with or without DOX and FGF. Data are depicted as mean \pm SD. * $P < 0.05$. ** $P < 0.01$.

classes of pluripotent cells also showed a rapid growth rate and no sign of senescence beyond 50 passages. However, the up-regulation of KLF4 and OCT4 in the whole ICM may produce pluripotent cells that lack homogenous outgrowth because the cells might be derived from different blastomeres with different integration of exogenous transcriptional factors. For this reason, we first transfected the PEFs with reprogramming factors and then conducted the SCNT to generate naive-like ESCs from ICMs with homogenization. We routinely used trypsin to passage porcine ESCs for more than 130 passages, and they demonstrated good cell viability.

The success of porcine ESC establishment is affected by several factors, including the main culture medium and the small molecules used. Culture medium has profound effects on cell identity because the cell fate transition can be induced or promoted by switching different culture medium. The research by Gu *et al.* (22) showed that H9 cells were quickly converted to naive states with an alternative culture medium, and colonies in the medium containing N2B27 looked more domed when compared with colonies in the medium containing only KOSR. N2B27 medium was used to isolate rat ESCs (5) and was successfully used

in the establishment of naive rat ESCs when combined with the Erk inhibitor PD0325901 and the Gsk3 inhibitor CHIR99021 (6). Combining these 2 inhibitors with LIF provides a defined culture system that is effective for all strains of mice and rats tested, supporting efficient ESC derivation and clonal expansion from dissociated cells (35). The activin receptor inhibitor SB can increase bone morphogenetic protein (BMP) signaling activity (36), and BMP4 has positive effects on mESCs in terms of self-renewal and resistance to differentiation (37), whereas human ESCs rapidly differentiate when exposed to BMP4 (38). Our results showed that the naive-like ESCs could be efficiently generated in LBX medium that contained N2B27, supplemented with CHIR99021, PD0325901, and SB, and combined with LIF.

The naive-like ESCs derived in our lab have characteristics very similar to those of naive mouse PSCs. In mice and pigs, SSEA-1 is ontogenetically expressed in the ICM; however, in humans, it is expressed in the morulae and trophoblasts instead (7). Mouse and human ESCs also have a distinct expression pattern of cell surface markers that characterize the undifferentiated state (39) because SSEA-1 is expressed in mouse ESCs but is absent in human

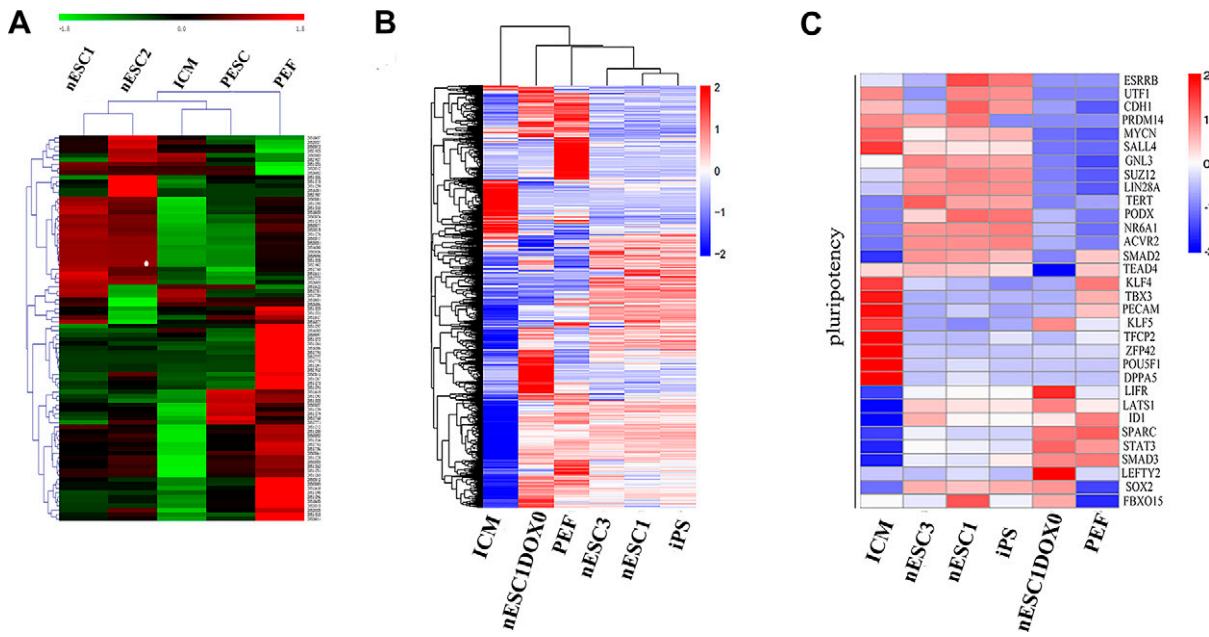


Figure 7. MicroRNA expression using Affymetrix microarrays and RNA-seq analysis of nESCs. *A*) Two-color heatmap representation of microRNA expression data derived from Affymetrix gene chip analysis. Each row represents the expression of a single microRNA, and columns indicate samples. nESC1, nESC line 1 at passage 13; nESC2, nESC line 2 at passage 14. *B*) Heatmap showing scaled expression values of 25,492 differentially expressed genes [\log_2 (fold change) >3 , adjusted P value <0.05] among the 6 cell types. *C*) Expression heatmap of pluripotency genes for each cell type. The results are shown by the Z score of the FPKMs of all samples for each gene. FPKMs, fragments per kilo-base of exon per million fragments mapped; iPSC, porcine iPSCs at passage 20; nESC1, nESC line 1 at passage 24; nESC3, nESC line 3 at passage 24; nESCIDOX0, nESC line 1 at passage 27 cultured without DOX; PEF, porcine embryonic fibroblast cells at passage 3.

ESCs. The surface marker SSEA-1 was readily detected in the nESCs, and the protein expression of SSEA-1 was also confirmed by immunofluorescence and Western blotting. Activation of STAT3 is essential for mouse ESC self-renewal mediated by signaling through LIF or gp130 receptors (40). Interestingly, LIF or STAT3 signaling fails to maintain self-renewal of mouse epiblast-derived stem cells (EpiSCs) and human ESCs (8, 41, 42). Our results demonstrated that the nESCs expressed the LIF receptors (LIFRs) and their subunits, LIFR- α , LIFR- β , and GP130. A hallmark of female ESCs and the early epiblast is that both X chromosomes are active. Upon proper differentiation, 1 X chromosome then becomes silenced (5). Our finding showed that the conversion of nESCs from female cell lines into a primed state is associated with up-regulation of XIST and a decrease in the fluorescence intensity of the H3K27me3 spot in the nESCs when compared with the rpESCs. We also showed that nESCs can spontaneously differentiate into cells expressing markers of the 3 somatic germ layers, and they can also respond to a differentiation protocol for inducing the differentiation of neural and kidney precursors.

The most important characteristic of the stem cell naive state is its LIF pathway dependence. LIF and bFGF, respectively, play important roles in maintaining mouse and human ESC pluripotency. The LIF signaling triggers the activation of the transcription factor Stat3, thereby allowing ESCs to maintain their undifferentiated state and self-renewal capacity (40). We demonstrated that nESCs depend on LIF signaling for self-renewal, and that the LIF-JAK-STAT3 pathway is essential for pluripotency. The

medium without LIF did not support stable cell growth because LIF withdrawal over 2 successive passages resulted in colonies that displayed overt signs of differentiation with the loss of compact morphology, and the differentiation was also much more pronounced with the inclusion of a JAK1 inhibitor. The nESCs were also LIF-dependent, as evident by the protein expression of phosphorylated STAT3. By contrast, blocking of the FGF pathway failed to interfere with the self-renewal and pluripotency of nESCs, indicating that this pathway does not play a central role in sustaining pluripotency in nESCs.

At present, the major issues of iPSC techniques are an insufficient initiation of endogenous transcription factors and the difficulty in completely silencing exogenous transcription factors, both of which obstruct the application of iPSCs. Human ESCs have reached a new pluripotent state with similar characters of mouse ESCs by exogenous expression of 3 pluripotent factors (KLF4, OCT4, SOX2), but maintenance of naive PSC lines for longer than 20 passages without the expression of exogenes has not been possible (9). We showed that the nESC line 4 survived at least 10 generations of culture after DOX was removed and that endogenous SOX2 was activated, although the other 3 exogenous transcription factors could not be completely silenced. Recently, the research on porcine iPSCs indicated that efficient transgene silencing is essential for the derivation of naive iPSC lines and is a prerequisite for normal cell differentiation (43). Therefore, the main problem of the cell lines established in our lab may also be insufficient initiation of the endogenous transcription factors and incomplete silencing of

exogenous transcription factors. Next, we intend to use the vector carrying both a 2A-peptide-linked reprogramming cassette, c-MYC-KLF4-OCT4-SOX2-ires, and the loxP sites so that the exogenous reprogramming factors can be completely removed by using subsequent Cre-transfection after the stable ESC line is established.

The establishment and maintenance of ESC lines is much more complicated from porcine blastocysts than from mouse embryos or primate embryos. The key molecules and the appropriate levels of gene expression required to maintain the ground state of authentic porcine ESCs are still unknown. In mouse blastocysts, NANOG is expressed in conjunction with OCT4 and SOX2 to confer pluripotent properties to the ICM, whereas in the pig, the concerted expression of these factors is delayed until the epiblast stage (44). Consequently, identification of surrogate markers for the naivety of porcine ESCs is important. Our RNA-seq analysis showed significantly higher expression of OCT4, TBX3, REX-1, DPPA5, and KLF4 in ICMs than in our nESCs; therefore, the transfection of the 4 OSKM factors might not be sufficient to support porcine pluripotent cells in the naive state, and we need to test other transcription factors. Because the current culture conditions for porcine PSCs are not yet the optimal system, the identification of other culture conditions that enable porcine PSCs to assume an authentic naive state will be necessary. Further, the use of different exogenous factor combinations and small molecular inhibitors may also allow the *in vitro* production of transgene-independent and stable naive porcine pluripotent cells. ■

ACKNOWLEDGMENTS

The authors thank all the laboratory staff for help in ensuring the accuracy and completeness of all the data and Prof. Siqin Bao (Inner Mongolia University, Huhhot, China) for reading the manuscript. This work was supported by the National Natural Sciences Foundation of China (Grant 31371487) and a grant from the Jiangsu Key Laboratory of Xenotransplantation (BM2012116). The authors declare no conflicts of interest.

AUTHOR CONTRIBUTIONS

M. Zhang designed the study, performed the experiments, and drafted the manuscript; C. Wang and H. Jiang performed the experiments, analyzed the data, and prepared the manuscript; M. Liu and N. Yang performed the experiments; L. Zhao and D. Hou helped to perform the experiments regarding molecular biological technique; Y. Jin, Q. Chen, Y. Chen, and J. Wang provided much help collecting oocytes and performing somatic cell nuclear transfer; Y. Dai provided suggestions on experimental design and revised the manuscript; R. Li designed the study and edited and finally approved the manuscript; and all authors read and approved the final manuscript.

REFERENCES

- Nichols, J., and Smith, A. (2009) Naive and primed pluripotent states. *Cell Stem Cell* **4**, 487–492
- Hanna, J. H., Saha, K., and Jaenisch, R. (2010) Pluripotency and cellular reprogramming: facts, hypotheses, unresolved issues. *Cell* **143**, 508–525
- Evans, M. J., and Kaufman, M. H. (1981) Establishment in culture of pluripotential cells from mouse embryos. *Nature* **292**, 154–156
- Martin, G. R. (1981) Isolation of a pluripotent cell line from early mouse embryos cultured in medium conditioned by teratocarcinoma stem cells. *Proc. Natl. Acad. Sci. USA* **78**, 7634–7638
- Buehr, M., Meek, S., Blair, K., Yang, J., Ure, J., Silva, J., McLay, R., Hall, J., Ying, Q. L., and Smith, A. (2008) Capture of authentic embryonic stem cells from rat blastocysts. *Cell* **135**, 1287–1298
- Li, P., Tong, C., Mehrian-Shai, R., Jia, L., Wu, N., Yan, Y., Maxson, R. E., Schulze, E. N., Song, H., Hsieh, C. L., Pera, M. F., and Ying, Q. L. (2008) Germline competent embryonic stem cells derived from rat blastocysts. *Cell* **135**, 1299–1310
- Fujishiro, S. H., Nakano, K., Mizukami, Y., Azami, T., Arai, Y., Matsunari, H., Ishino, R., Nishimura, T., Watanabe, M., Abe, T., Furukawa, Y., Umeyama, K., Yamanaka, S., Ema, M., Nagashima, H., and Hanazono, Y. (2013) Generation of naive-like porcine-induced pluripotent stem cells capable of contributing to embryonic and fetal development. *Stem Cells Dev.* **22**, 473–482
- Brons, I. G., Smithers, L. E., Trotter, M. W., Rugg-Gunn, P., Sun, B., Chuva de Sousa Lopes, S. M., Howlett, S. K., Clarkson, A., Ahrlund-Richter, L., Pedersen, R. A., and Vallier, L. (2007) Derivation of pluripotent epiblast stem cells from mammalian embryos. *Nature* **448**, 191–195
- Hanna, J., Cheng, A. W., Saha, K., Kim, J., Lengner, C. J., Soldner, F., Cassady, J. P., Muffat, J., Carey, B. W., and Jaenisch, R. (2010) Human embryonic stem cells with biological and epigenetic characteristics similar to those of mouse ESCs. *Proc. Natl. Acad. Sci. USA* **107**, 9222–9227
- Huang, K., Maruyama, T., and Fan, G. (2014) The naive state of human pluripotent stem cells: a synthesis of stem cell and preimplantation embryo transcriptome analyses. *Cell Stem Cell* **15**, 410–415
- Nichols, J., and Smith, A. (2011) The origin and identity of embryonic stem cells. *Development* **138**, 3–8
- Tesar, P. J., Chennoweth, J. G., Brook, F. A., Davies, T. J., Evans, E. P., Mack, D. L., Gardner, R. L., and McKay, R. D. (2007) New cell lines from mouse epiblast share defining features with human embryonic stem cells. *Nature* **448**, 196–199
- Haraguchi, S., Kikuchi, K., Nakai, M., and Tokunaga, T. (2012) Establishment of self-renewing porcine embryonic stem cell-like cells by signal inhibition. *J. Reprod. Dev.* **58**, 707–716
- Notarianni, E., Galli, C., Laurie, S., Moor, R. M., and Evans, M. J. (1991) Derivation of pluripotent, embryonic cell lines from the pig and sheep. *J. Reprod. Fertil. Suppl.* **43**, 255–260
- Notarianni, E., Laurie, S., Moor, R. M., and Evans, M. J. (1990) Maintenance and differentiation in culture of pluripotential embryonic cell lines from pig blastocysts. *J. Reprod. Fertil. Suppl.* **41**, 51–56
- Piedrahita, J. A., Anderson, G. B., and Bondurant, R. H. (1990) On the isolation of embryonic stem cells: comparative behavior of murine, porcine and ovine embryos. *Theriogenology* **34**, 879–901
- Chen, L. R., Shiu, Y. L., Bertolini, L., Medrano, J. F., BonDurant, R. H., and Anderson, G. B. (1999) Establishment of pluripotent cell lines from porcine preimplantation embryos. *Theriogenology* **52**, 195–212
- Telugu, B. P., Ezashi, T., Sinha, S., Alexenko, A. P., Spate, L., Prather, R. S., and Roberts, R. M. (2011) Leukemia inhibitory factor (LIF)-dependent, pluripotent stem cells established from inner cell mass of porcine embryos. *J. Biol. Chem.* **286**, 28948–28953
- Gafni, O., Weinberger, L., Mansour, A. A., Manor, Y. S., Chomsky, E., Ben-Yosef, D., Kalma, Y., Viukov, S., Maza, I., Zviran, A., Rais, Y., Shipony, Z., Mukamel, Z., Krupalnik, V., Zerbib, M., Geula, S., Caspi, I., Schneir, D., Schwartz, T., Gilad, S., Amann-Zalcenstein, D., Benjamin, S., Amit, I., Tanay, A., Massarwa, R., Novershtern, N., and Hanna, J. H. (2013) Derivation of novel human ground state naive pluripotent stem cells. *Nature* **504**, 282–286; erratum: 520, 710
- Takashima, Y., Guo, G., Loos, R., Nichols, J., Ficz, G., Krueger, F., Oxley, D., Santos, F., Clarke, J., Mansfield, W., Reik, W., Bertone, P., and Smith, A. (2014) Resetting transcription factor control circuitry toward ground-state pluripotency in human. *Cell* **158**, 1254–1269; erratum: 162, 152–153
- Theunissen, T. W., Powell, B. E., Wang, H., Mitalipova, M., Faddah, D. A., Reddy, J., Fan, Z. P., Maetzel, D., Ganz, K., Shi, L., Lungjangwa, T., Imsoonthornruksa, S., Stelzer, Y., Rangarajan, S., D'Alessio, A.,

- Zhang, J., Gao, Q., Dawlaty, M. M., Young, R. A., Gray, N. S., and Jaenisch, R. (2014) Systematic identification of culture conditions for induction and maintenance of naive human pluripotency. *Cell Stem Cell* **15**, 471–487; erratum: 524–526
22. Gu, Q., Hao, J., Zhao, X. Y., Li, W., Liu, L., Wang, L., Liu, Z. H., and Zhou, Q. (2012) Rapid conversion of human ESCs into mouse ESC-like pluripotent state by optimizing culture conditions. *Protein Cell* **3**, 71–79
23. Gu, Q., Hao, J., Hai, T., Wang, J., Jia, Y., Kong, Q., Wang, J., Feng, C., Xue, B., Xie, B., Liu, S., Li, J., He, Y., Sun, J., Liu, L., Wang, L., Liu, Z., and Zhou, Q. (2014) Efficient generation of mouse ESCs-like pig induced pluripotent stem cells. *Protein Cell* **5**, 338–342
24. Ezashi, T., Telugu, B. P. V. L., Alexenko, A. P., Sachdev, S., Sinha, S., and Roberts, R. M. (2009) Derivation of induced pluripotent stem cells from pig somatic cells. *Proc. Natl. Acad. Sci. USA* **106**, 10993–10998
25. Takasato, M., Er, P. X., Becroft, M., Vanslambrouck, J. M., Stanley, E. G., Elefanty, A. G., and Little, M. H. (2014) Directing human embryonic stem cell differentiation towards a renal lineage generates a self-organizing kidney. *Nat. Cell Biol.* **16**, 118–126
26. Kawasaki, H., Mizuseki, K., Nishikawa, S., Kaneko, S., Kuwana, Y., Nakanishi, S., Nishikawa, S. I., and Sasai, Y. (2000) Induction of midbrain dopaminergic neurons from ES cells by stromal cell-derived inducing activity. *Neuron* **28**, 31–40
27. Hou, D. R., Jin, Y., Nie, X. W., Zhang, M. L., Ta, N., Zhao, L. H., Yang, N., Chen, Y., Wu, Z. Q., Jiang, H. B., Li, Y. R., Sun, Q. Y., Dai, Y. F., and Li, R. F. (2016) Derivation of porcine embryonic stem-like cells from *in vitro*-produced blastocyst-stage embryos. *Sci. Rep.* **6**, 25838
28. Keller, G. M. (1995) *In vitro* differentiation of embryonic stem cells. *Curr. Opin. Cell Biol.* **7**, 862–869
29. Anderson, G. B., Choi, S. J., and Bondurant, R. H. (1994) Survival of porcine inner cell masses in culture and after injection into blastocysts. *Theriogenology* **42**, 204–212
30. Strojek, R. M., Reed, M. A., Hoover, J. L., and Wagner, T. E. (1990) A method for cultivating morphologically undifferentiated embryonic stem cells from porcine blastocysts. *Theriogenology* **33**, 901–913
31. Li, M., Zhang, D., Hou, Y., Jiao, L., Zheng, X., and Wang, W. H. (2003) Isolation and culture of embryonic stem cells from porcine blastocysts. *Mol. Reprod. Dev.* **65**, 429–434
32. Li, M., Ma, W., Hou, Y., Sun, X. F., Sun, Q. Y., and Wang, W. H. (2004) Improved isolation and culture of embryonic stem cells from Chinese miniature pig. *J. Reprod. Dev.* **50**, 237–244
33. Kim, H. S., Son, H. Y., Kim, S., Lee, G. S., Park, C. H., Kang, S. K., Lee, B. C., Hwang, W. S., and Lee, C. K. (2007) Isolation and initial culture of porcine inner cell masses derived from *in vitro*-produced blastocysts. *Zygote* **15**, 55–63
34. Kim, S., Kim, J. H., Lee, E., Jeong, Y. W., Hossein, M. S., Park, S. M., Park, S. W., Lee, J. Y., Jeong, Y. I., Kim, H. S., Kim, Y. W., Hyun, S. H., and Hwang, W. S. (2010) Establishment and characterization of embryonic stem-like cells from porcine somatic cell nuclear transfer blastocysts. *Zygote* **18**, 93–101
35. Ying, Q. L., Wray, J., Nichols, J., Batlle-Morera, L., Doble, B., Woodgett, J., Cohen, P., and Smith, A. (2008) The ground state of embryonic stem cell self-renewal. *Nature* **453**, 519–523
36. Xu, R. H., Sampsell-Barron, T. L., Gu, F., Root, S., Peck, R. M., Pan, G., Yu, J., Antosiewicz-Bourget, J., Tian, S., Stewart, R., and Thomson, J. A. (2008) NANOG is a direct target of TGF β /activin-mediated SMAD signaling in human ESCs. *Cell Stem Cell* **3**, 196–206
37. Ying, Q. L., Nichols, J., Chambers, I., and Smith, A. (2003) BMP induction of Id proteins suppresses differentiation and sustains embryonic stem cell self-renewal in collaboration with STAT3. *Cell* **115**, 281–292
38. Xu, R. H., Chen, X., Li, D. S., Li, R., Addicks, G. C., Glennon, C., Zwaka, T. P., and Thomson, J. A. (2002) BMP4 initiates human embryonic stem cell differentiation to trophoblast. *Nat. Biotechnol.* **20**, 1261–1264
39. Ginis, I., Luo, Y., Miura, T., Thies, S., Brandenberger, R., Gerecht-Nir, S., Amit, M., Hoke, A., Carpenter, M. K., Itskovitz-Eldor, J., and Rao, M. S. (2004) Differences between human and mouse embryonic stem cells. *Dev. Biol.* **269**, 360–380
40. Niwa, H., Burdon, T., Chambers, I., and Smith, A. (1998) Self-renewal of pluripotent embryonic stem cells is mediated via activation of STAT3. *Genes Dev.* **12**, 2048–2060
41. Humphrey, R. K., Beattie, G. M., Lopez, A. D., Bucay, N., King, C. C., Firpo, M. T., Rose-John, S., and Hayek, A. (2004) Maintenance of pluripotency in human embryonic stem cells is STAT3 independent. *Stem Cells* **22**, 522–530
42. Daheron, L., Opitz, S. L., Zaehres, H., Lensch, M. W., Andrews, P. W., Itskovitz-Eldor, J., and Daley, G. Q. (2004) LIF/STAT3 signaling fails to maintain self-renewal of human embryonic stem cells. *Stem Cells* **22**, 770–778; erratum: 25, 3273
43. Du, X., Feng, T., Yu, D., Wu, Y., Zou, H., Ma, S., Feng, C., Huang, Y., Ouyang, H., Hu, X., Pan, D., Li, N., and Wu, S. (2015) Barriers for deriving transgene-free pig iPS cells with episomal vectors. *Stem Cells* **33**, 3228–3238
44. Alberio, R., Croxall, N., and Allegrucci, C. (2010) Pig epiblast stem cells depend on activin/nodal signaling for pluripotency and self-renewal. *Stem Cells Dev.* **19**, 1627–1636

Received for publication December 24, 2018.

Accepted for publication April 23, 2019.